A Mechanistic Study of Oscillations and Bistability in the Briggs-Rauscher Reaction

Patrick De Kepper and Irving R. Epstein*

Contribution from the Department of Chemistry, Brandeis University, Waltham, Massachusetts 02254. *Received July 27, 1981*

Abstract: A ten-step mechanism has been developed for the Briggs-Rauscher system which contains iodate, hydrogen peroxide, malonic acid, and manganese(II) in acidic solution. The model is qualitatively identical with, though it differs quantitatively from, that proposed independently by Noyes and Furrow. It also bears strong similarities to the mechanistic suggestions of Cooke. Extensive numerical simulations of the reaction in a flow reactor show that the model predicts the observed topology of the "cross-shaped phase diagram" in which both bistability and oscillations appear as the input flows of the reactant species are varied. The observed hysteresis in the steady-state iodine concentration as a function of I_2 flow and a variety of other dynamic behavior are also calculated in agreement with experiment. The remaining discrepancies between theory and experiment appear to result from an overestimation in the model of the stability of the nonradical steady state. A possible remedy for this problem is suggested.

The Briggs-Rauscher (BR) reaction,[1] in which the acidic oxidation of malonic acid by a mixture of hydrogen peroxide and iodate is catalyzed by manganous ion, is best known as the most visually impressive of the chemical oscillators. Under appropriate conditions and with the addition of a starch indicator, at room temperature a stirred batch solution goes through 15 or more cycles of colorless-gold-blue before expiring as a purplish solution with a strong odor of iodine.

The BR reaction, however, exhibits a far richer collection of nonlinear dynamic phenomena than simple oscillation. In a flow reactor, complex oscillations[2] as well as multiple stable states[3] accompanied by a variety of bifurcation and hysteresis phenomena have been observed.[2,4]

The BR system was discovered some 8 years ago and is a hybrid of two other chemical oscillators, the Belousov-Zhabotinskii (BZ)[5] and the Bray-Liebhafsky (BL) reactions,[6] for which detailed mechanisms have been proposed and numerically evaluated.[7,8] It is therefore surprising that until quite recently there had been no quantitative and very little qualitative discussion of the mechanism of the BR reaction.

Cooke[9] has studied the BR and related systems experimentally and has made a number of mechanistic suggestions based on his results. No quantitative comparison between theory and experiment was carried out. More recently, Furrow and Noyes[10] have conducted a systematic study of the reaction, investigating the kinetics of the reacting species taken two and three at a time. These authors have proposed a skeleton mechanism and have estimated rate constants for the elementary steps in that mechanism. They have also reported a single numerical simulation[10c] with their model which shows that it can indeed give rise to oscillations.

In this paper, we use a broad range of experimental data obtained mainly, but not exclusively, under flow conditions, to guide the construction of a mechanism for the BR reaction. Although we approach the problem from a rather different point of view, we have independently arrived at a mechanism similar to that of Cooke and nearly identical with that of Furrow and Noyes. We have carried out extensive calculations with our mechanism in an attempt to simulate not only the oscillatory behavior, but the multistability, hysteresis, and bifurcation phenomena as well. We find qualitative agreement with nearly all of the observed phenomena and quantitative agreement with some. Most of the discrepancies which remain between our calculations and the experimental results can be attributed to a single weakness of the model—its exaggeration of the stability of the nonradical steady state of the system. We suggest how the mechanism might be augmented to correct this failing.

Modifications of the BR system in which malonic acid is replaced by related organic species[1,9,11] are also known to oscillate. In particular, Furrow[11] has carried out a careful study of the BR reaction with methylmalonic acid and has found a significant lengthening of the oscillation period over that of the malonic acid system. By introducing Furrow's experimentally determined rate parameters for the methylmalonic acid-iodine reaction at the appropriate point in our model, we show that it indeed predicts the observed increase in the period of oscillation.

Experimental Studies

Since the initial study of Briggs and Rauscher[1] in 1973, the BR system has been the subject of a variety of investigations.

Cooke[9] has looked at the BR reaction and the related system with malonic acid replaced by acetone under batch conditions. He has studied the dependence of the period and of the redox potential trace on the concentrations of the constituent species. He has also examined the behavior of the inorganic components (hydrogen peroxide, iodate, manganese) and the effect of Cu(II) and Cl^- ions on these reactions.

Furrow and Noyes[10a,b] have also attempted to simplify the BR system by examining several subsystems in some detail in a batch configuration. They first probe the set of inorganic reactions and then consider the role of various organic substrates as replacements for malonic acid in an effort to elucidate the mechanisms of the component reactions.

The most extensive experiments on the BR system have been carried out by De Kepper et al.[2,4,12] in a continuous-flow stirred-tank reactor (CSTR). These more phenomenologically oriented studies probed a portion of the phase diagram in the constraint space defined by iodate, hydrogen peroxide, malonic acid, temperature, and residence time. A

(1) Briggs, T. C.; Rauscher, W. C. *J. Chem. Educ.* **1973**, *50*, 496.
(2) (a) De Kepper, P.; Pacault, A.; Rossi, A. *C. R. Hebd. Acad. Sci., Ser. C* **1976**, *282C*, 199-204. (b) Pacault, A.; De Kepper, P.; Hanusse, P.; Rossi, A. *Ibid.* **1975**, *281C*, 215-220. (c) De Kepper, P.; Pacault, A. *Ibid.* **1978**, *286C*, 437-441.
(3) We employ the term "stable state" to mean a dynamic state to which the system will return after a small perturbation. Such states may be either steady (concentrations constant) or oscillatory (concentrations vary periodically).
(4) Pacault, A.; Hanusse, P.; De Kepper, P.; Vidal, C.; Boissonade, J. *Acc. Chem. Res.* **1976**, *9*, 439-445.
(5) Belousov, B. P. "Ref. *Radiats.* Med., 1958"; Medgiz: Moscow, 1959; p 145. Zhabotinsky, A. M. *Dokl. Akad. Nauk SSSR* **1964**, *157*, 392-395.
(6) Bray, W. C. *J. Am. Chem. Soc.* **1921**, *43*, 1262-1267. Liebhafsky, H. A. *Ibid.* **1931**, *53*, 896-911.
(7) Edelson, D.; Noyes, R. M.; Field, R. J. *Int. J. Chem. Kinet.* **1979**, *11*, 156-164.
(8) Edelson, D.; Noyes, R. M. *J. Phys. Chem.* **1979**, *83*, 212-220.
(9) (a) Cooke, D. O. *Inorg. Chim. Acta* **1979**, *37*, 259-265. (b) *Int. J. Chem. Kinet.* **1980**, *12*, 671-681. (c) *Ibid.* **1980**, *12*, 683-698.
(10) (a) Furrow, S. D.; Noyes, R. M. *J. Am. Chem. Soc.*, part 1 in this issue. (b) *Ibid.*, part 2 in this issue. (c) Noyes, R. M.; Furrow, S. D. *Ibid.*, part 3 in this issue.
(11) Furrow, S. D., *J. Phys. Chem.*, submitted for publication.
(12) (a) De Kepper, P. Ph.D. Thesis, Bordeaux, France, 1978. (b) De Kepper, P., unpublished observations.

0002-7863/82/1504-0049$01.25/0

wealth of spectacular phenomena was revealed.

Different types of simple and complex oscillations as well as transitions among these and various steady states were observed. The responses monitored in these experiments were the absorbance at 460 nm, a measure of the I_2 concentration in the reactor, and the potential of a platinum electrode, primarily sensitive to the iodide concentration.

Roux and Vidal[13] carried out a single experiment in which the outputs of different sensors were fed into a computer for further analysis. Simultaneous oscillations of $[I^-]$, $[I_2]$, $[I_3^-]$, [iodomalonic acid], and $[O_2]$ are reported.

It is these flow experiments, and in particular their determination of the regions of the constraint space in which the system exhibits oscillations in connection with a neighboring region of bistability between two steady states, that we shall employ as the primary test of our mechanism. We shall occasionally refer to the results of batch experiments as well when they provide a relevant comparison between theory and experiment.

Construction of the Mechanism

Choice of Reactions. Briggs and Rauscher[1] note the presence of manganese (or cerium) and malonic acid in both BR and BZ reactions and suggest that the similarity between the two reactions results from the role of malonic acid as a halogen consumer and halide producer in both systems. Roux and Vidal,[13] on the basis of a careful analysis of the rates of production and consumption of various halogen-containing species in the oscillating BR system in comparison with the BZ and BL oscillators, conclude that the siimilarity between the BR and BZ systems is even more fundamental. They also observe that while MA serves as the major source of halide in the BZ reaction, in the BR system it appears to serve primarily as a halogen sink.

Extensive studies of the BZ[14] and BR[12,15] reactions in a stirred tank reactor (CSTR) reveal further parallels in their dynamic behavior. Most strikingly, under appropriate conditions both systems exhibit a region of bistability between two different steady states, regions in which each state is uniquely stable and a region of oscillations, all of which are linked in a characteristic "cross-shaped phase diagram".[15] In both reactions, the steady states differ in their halide concentrations by several orders of magnitude. In the BZ reaction, the low halide state is recognized[15] as being dominated by radical processes. The low halide BR state is characterized by a high I_2 concentration and an increase in the rate of O_2 evolution suggesting, by analogy with Noyes and Sharma's analysis of the BL reaction, a rapid decomposition of H_2O_2 via a radical process.

In both systems large amplitude oscillating states show complex secondary small amplitude oscillations about the low halide pseudo steady state.[2] Furthermore, transitions from the high halide state to the oscillatory state show subcritical bifurcation[17] on increasing the malonic acid flow in both the BR and BZ reactions.[12,14b,15]

These resemblances in the dynamic behavior suggest that our skeleton mechanism should contain a series of steps which mimic the essential steps of the FKN mechanism[16] which has been so successful in predicting a wealth of phenomena in the BZ system.

The FKN mechanism contains five reactions which summarize the chemistry of the principal bromine-containing species in the BZ reaction, Br^-, Br_2, HOBr, $HBrO_2$, BrO_2, and BrO_3^-. To characterize the iodine chemistry in the BR system, we adopt the same set of five elementary steps (eq 1–5) with bromine replaced by iodine.

$$2H^+ + I^- + IO_3^- = HOI + HIO_2 \quad (1)$$

$$H^+ + HIO_2 + I^- = 2HOI \quad (2)$$

$$HOI + I^- + H^+ = I_2 + H_2O \quad (3)$$

$$HIO_2 + IO_3^- + H^+ = 2IO_2 + H_2O \quad (4)$$

$$2HIO_2 = HOI + IO_3^- + H^+ \quad (5)$$

Along with a number of other authors,[9,10a] we have observed that the slow decomposition of hydrogen peroxide by iodate is greatly accelerated by the presence of manganous salts. The oxidation of H_2O_2 by iodine-containing species should thus involve Mn(II) and Mn(III) through a radical process. This view is also consistent with Briggs and Rauscher's observation[1] that oscillations may occur in the absence of a metal ion catalyst, but only at greatly increased $[H_2O_2]$ and $[H^+]$.

The key radical species in the FKN mechanism is BrO_2, which leads to the autocatalytic production of $HBrO_2$. A similar autocatalytic production of HIO_2 can be obtained in our mechanism by introducing reaction 6.[19]

$$IO_2 + Mn^{2+} + H_2O = HIO_2 + MnOH^{2+} \quad (6)$$

In the BZ reaction with both cerium and manganese, oscillations amounting to 10% or more of the initial catalyst concentration have been observed.[14,16] Experiments on the BR reaction have failed to detect changes in the Mn(II) concentration or measurable amounts of Mn(III), even using paramagnetic resonance techniques sensitive to 0.3% changes in [Mn(II)].[12b]

The regeneration of Ce(III) in the BZ reaction results from the oxidation of malonic acid and its derivatives by Ce(IV).[16] The analogous reaction in the BR system is apparently too slow to yield Mn(II) at a significant rate and whatever Mn(III) does form must be reduced in a rapid reaction probably with H_2O_2, which is present in high concentration. We thus add to our mechanism reaction 7 as the simplest step of this type. While further radicals

$$H_2O_2 + MnOH^{2+} = HO_2 + Mn^{2+} + H_2O \quad (7)$$

such as OH, IO, etc. might be postulated, the simplest chain-termination step consistent with the stability of the various radical species is

$$2HO_2 = H_2O_2 + O_2 \quad (8)$$

Preliminary calculations using eq 1–8 confirmed that this set of reactions does give rise to bistability under appropriate flow conditions. We were thus assured that our initial estimates of the rate constants and the dynamic structure of this part of our model were compatible with a key experimental phenomenon.

In order to obtain oscillations as well as bistability, it is necessary to introduce a means of regenerating iodide, one of the principal oscillatory species in the BR reaction. The equilibrium constants for reactions 2 and 3 are such that the reverse reactions cannot serve as major sources of I^-. An obvious source of iodide is the iodination of malonic acid

$$I_2 + MA = IMA + I^- + H^+ \quad (9)$$

where MA and IMA represent malonic and iodomalonic acids, respectively. An analogous step provides the major source of bromide in the BZ reaction. A second iodide-producing reaction

$$HOI + H_2O_2 = I^- + O_2 + H^+ + H_2O \quad (10)$$

was also introduced. While hydrogen peroxide surely interacts with other iodine species as well, reaction 10 is probably the most significant such reaction under the usual reaction conditions.

Several other steps such as

$$HO_2 + I_2 \overset{[H_2O_2,\ H^+]}{=} IO + (1-\alpha)HOI + \alpha I^- + O_2 \quad (11)$$

and

(13) Roux, J. C.; Vidal, C. "Synergetics - Far from Equilibrium"; Pacault, A., Vidal C., Eds.; Springer-Verlag: Berlin, 1979; pp 47–50.

(14) (a) De Kepper, P.; Rossi, A.; Pacault, A. *C. R. Hebd. Acad. Sci., Ser. C* **1976**, *283C*, 371–375. (b) De Kepper, P.; Boissonade, J. *J. Chem. Phys.* **1981**, *75*, 189–195.

(15) Boissonade, J.; De Kepper, P. *J. Phys. Chem.* **1980**, *84*, 501–506.

(16) Field, R. J.; Körös, E.; Noyes, R. M. *J. Am. Chem. Soc.* **1972**, *94*, 8649–8664.

(17) Marsden, J.; McCracken, M. "The Hopf Bifurcation and its Applications"; Springer-Verlag: New York, 1977.

(18) Graziani, K. R.; Hudson, J. L.; Schmitz, R. A. *Chem. Eng. J.* **1976**, *12*, 9.

(19) We write the manganic species as $MnOH^{2+}$, since the equilibrium constant for the hydrolysis reaction $Mn^{3+} + H_2O = MnOH^{2+} + H^+$ is 0.93 M at 25 °C (Davies, G.; Kirschenbaum, L. J.; Kustin, K. *Inorg. Chem.* **1968**, *7*, 146–154). At a typical $[H^+]$ for the BR system of 5×10^{-2} M, we have $[Mn(OH)^{2+}]/[Mn^{3+}] \approx 20$.

$$IO + IO_3^- + H^+ = IO_2 + HIO_2 \quad (12)$$

were introduced in the early stages of this work as a convenient way of summarizing several possible radical pathways. Since inclusion of these reactions increased the complexity of the model, both in terms of the number of equations and the number of independent species, without producing better agreement between the calculated and experimental results, these steps were dropped from the mechanism.

We are thus left with the ten steps ((1)–(10)). As we discuss in the next section, rate constants for these steps were chosen where possible from experimental data in the literature. The remaining parameters, k_2, k_4, k_5, and k_6, were then varied in an attempt to optimize agreement with two major dynamical features: (a) the cross-shaped phase diagram[15] in which bistability and oscillations give way to unique steady states as input species concentrations are varied, and (b) the "inverse regulation" of iodine[2c] in which the I_2 concentration in the reactor drops dramatically as the iodine flow is increased above a critical value.

Values of Rate Constants. Having chosen what we believe to be a plausible set of component reactions, we now require a rate law and corresponding rate constants for each of these steps in order to simulate numerically the experimental data. We discuss sequentially each of the steps ((1)–(10)) in our mechanism with respect to its rate expression.

Reaction 1. This reaction constitutes the initial step in the Dushman reaction[20] and has been studied experimentally by Furuichi and Liebhafsky[21] at an iodide concentration of 10^{-9} M maintained by addition of AgI and $AgNO_3$. Using a quasi-empirical rate law of the form

$$v_1 = -d[IO_3^-]/dt = k_1[H^+]^2[I^-][IO_3^-] \quad (V1)$$

they obtain a value of $k_1 = 1.43 \times 10^3$ M^{-3} s^{-1} at 25 °C. Noyes and Furrow[10c] employ the same value. By working at such a low iodide concentration, Furuichi and Liebhafsky were able to eliminate the effects of the term in the rate law for the Dushman reaction which is second order in $[I^-]$ and which presumably arises from more complex processes. Under the usual conditions for the BR reaction, $[HIO_2]$ and [HOI] are sufficiently low that the reverse of reaction 1 may be neglected.

Reaction 2. Since no direct experimental measurement has been made of the rate of this reaction, a rate constant was estimated by analogy with the corresponding bromine chemistry.

The forward and reverse rate constants for reaction 13 are taken

$$H^+ + HBrO_2 + Br^- = 2HOBr \quad (13)$$

in the FKN model[7] as 2.0×10^9 M^{-2} s^{-1} and 5.0×10^{-5} M^{-1} s^{-1}, respectively. These values have also been employed for reaction 13 by Bar-Eli and co-workers[22] in several numerical investigations of bromate-containing systems. In their study of the BR reaction, Furrow and Noyes suggest rate constants $k_2 = 5.4 \times 10^8$ M^{-2} s^{-1} and $k_{-2} = 90$ M^{-1} s^{-1} for reaction 2 in the IO_3^-–I_2O_2–Mn^{2+}–H^+ subsystem and $k_2 = 2 \times 10^9$ M^{-2} s^{-1} for the full system. The latter value has also been employed in numerical simulation of the BL reaction.[8]

Since the experimentally determined rates for the iodine reactions in steps 1 and 3 are about 10^3 faster than those for the corresponding bromine reactions, it seems reasonable to expect that $k_2^{HIO_2} > k_2^{HBrO_2}$. We thus took the rate law for step 2 to be

$$v_2 = -d[HIO_2]/dt = k_2[H^+][HIO_2][I^-] \quad (V2)$$

with $k_2 = 2 \times 10^{10}$ M^{-2} s^{-1}. The numerical simulations did not show significant improvement when k_2 was changed or when a reasonable non-zero value of k_{-2} was included.

Reaction 3. This reaction was studied by Eigen and Kustin[23] using a temperature-jump technique. At 20 °C, the rate law was found to be

$$v_3 = -d[HOI]/dt = k_3[H^+][HOI][I^-] - k_{-3}[I_2] \quad (V3)$$

with $k_3 = 3.1 \times 10^{12}$ M^{-2} s^{-1} and $k_{-3} = 2.2$ s^{-1}. Nearly identical values have been employed by Noyes and co-workers in their modeling of the BL and BR systems.[8,10c]

Reaction 4. No experimental data are available for this reaction. The relative instability of IO_2 should make reaction 4 less favorable than its bromine equivalent, for which the forward and reverse rates in the FKN scheme[7] are 7.3×10^3 M^{-2} s^{-1} and 1.7×10^7 M^{-1} s^{-1}, respectively. For reaction 4 in the BL system, Edelson and Noyes[8] give $k_4 = 1.06 \times 10^3$ M^{-2} s^{-1} and $k_{-4} = 4.64 \times 10^4$ M^{-1} s^{-1} at 50 °C, while Sharma and Noyes[24] suggest $k_4 = 7 \times 10^4$ M^{-2} s^{-1} and $k_4/k_{-4} = 4.2 \times 10^{-4}$ M^{-1}. Furrow and Noyes[10c] obtain values $k_4 = 1.5 \times 10^4$ M^{-2} s^{-1} and $k_{-4} = 1.6 \times 10^9$ M^{-1} s^{-1} in their model of the BR system and note that the features of the oscillation are very sensitive to these parameters.

We started from estimated values of $k_4 = 4 \times 10^2$ M^{-2} M^{-2} s^{-1} and $k_{-4} = 1.7 \times 10^7$ M^{-1} s^{-1} in the rate law

$$v_4 = -\frac{d[IO_3^-]}{dt} = k_4[H^+][IO_3^-][HIO_2] - k_{-4}[IO_2]^2 \quad (V4)$$

We found that improved agreement between the simulations and experiment was obtained with $k_4 = 7.3 \times 10^3$ M^{-2} s^{-1}. Note that because of the unknown potential of IO_2, the equilibrium constant for this reaction is not known. The value chosen for k_{-4} does not significantly influence our results.

Reaction 5. The forward and reverse rates for bromous acid disproportionation in the FKN model are estimated[7] as 4.0×10^7 M^{-1} s^{-1} and 2.0×10^{-10} M^{-1} s^{-1}, respectively. For reaction 5 in the BL system, Noyes and co-workers[8] have suggested $k_5 = 2 \times 10^9$ M^{-1} s^{-1} and $k_5 = 5.56 \times 10^7$ M^{-1} s^{-1}, $k_{-5} = 6.93 \times 10^{-6}$ M^{-2} s^{-1}. In their first paper on the BR reaction, Furrow and Noyes[10a] give $k_5 = 10^4$ M^{-1} s^{-1} and $k_{-5} = 0.86$ M^{-2} s^{-1}. Their mechanistic study,[10c] in which k_{-5} is set to zero, yields a value for k_5 of 45.3 M^{-1} s^{-1}. This value appears rather low, and the $[HIO_2]$ concentrations obtained in that work do seem unrealistically high.

We found the effects of including k_{-5} to be negligible. Starting from an initial estimate of $k_5 = 4 \times 10^6$ M^{-1} s^{-1}, we obtained an optimal value of $k_5 = 6 \times 10^5$ M^{-1} s^{-1} in the rate law

$$v_5 = -\tfrac{1}{2}d[HIO_2]/dt = k_5[HIO_2]^2 \quad (V5)$$

Reaction 6. The rate for this reaction was estimated from various radical–cation rate constants in the literature. The cerous–BrO_2 rate constant is given[7] as 1.5×10^5 M^{-2} s^{-1}, while Field[25] estimates that the rate constant for IO_2 plus Fe^{2+} is about 10^5 M^{-2} s^{-1}. Our calculations, in agreement with those of Noyes and Furrow,[10c] suggest that $k_6 = 1.0 \times 10^4$ M^{-1} s^{-1} in eq V6 gives the

$$v_6 = -d[IO_2]/dt = k_6[IO_2][Mn^{2+}] \quad (V6)$$

best results. In view of the extremely low concentration of Mn(III), the reverse reaction has been neglected.

Reaction 7. The rate law, taken from Davies et al.,[19] is

$$v_7 = -d[MnOH^{2+}]/dt = k_7[MnOH^{2+}][H_2O_2] \quad (V7)$$

with $k_7 = 3.2 \times 10^4$ M^{-1} s^{-1}. Inclusion of the reverse reaction has no effect on the simulations.

Reaction 8. This reaction is essentially irreversible. Sharma and Noyes'[24] value of $k_8 = 7.5 \times 10^5$ M^{-1} s^{-1} in rate law V8 was

$$v_8 = -\tfrac{1}{2}d[HO_2]/dt = k_8[HO_2]^2 \quad (V8)$$

adopted. Edwards[26] gives $k_8 = 5.4 \times 10^6$ M^{-1} s^{-1}, but so long as

(20) Dushman, S. J. *J. Phys. Chem.* **1904**, *8*, 453–482.
(21) Furuichi, R.; Liebhafsky, H. A. *Bull. Chem. Soc. Jpn.* **1975**, *48*, 745–750.
(22) Bar-Eli, K.; Noyes, R. M. *J. Phys. Chem.* **1978**, *82*, 1352–1359; Barkin, S.; Bixon, M.; Noyes, R. M.; Bar-Eli, K. *Int. J. Chem. Kinet.* **1977**, *9*, 841–862. Bar-Eli, K.; Geiseler, W., to be submitted for publication.
(23) Eigen, M.; Kustin, K. *J. Am. Chem. Soc.* **1962**, *84*, 1355–1361.
(24) Sharma, K. R.; Noyes, R. M. *J. Am. Chem. Soc.* *1976*, *98*, 4345–4361.
(25) Field, R. J.; Brummer, J. G. *J. Phys. Chem.* **1979**, *83*, 2328–2335.
(26) Edwards, J. O. In "Peroxide Reaction Mechanisms"; Edwards, J. O., Ed.; Interscience: New York, 1962, p 67.

Table I. Steady State Species Concentrations[a]

concn, M	I_2	I^-	HIO	HIO_2	IO_2	Mn(III)	MA
SSI	6.13×10^{-7}	2.94×10^{-8}	2.69×10^{-10}	3.18×10^{-10}	2.60×10^{-10}	9.85×10^{-13}	1.49×10^{-3}
SSII	7.42×10^{-4}	6.85×10^{-9}	1.38×10^{-6}	1.55×10^{-6}	7.40×10^{-7}	2.8×10^{-9}	9.93×10^{-4}

[a] Bistable composition with $[IO_3^-]_0 = 4 \times 10^{-2}$ M, $[I_2]_0 = 2.5 \times 10^{-6}$ M, all other constraints are as in Figure 1.

this reaction is rapid, the actual numerical value used is of little importance.

Reaction 9. This reaction takes place in two steps, enolization of the acid followed by iodination of the enol

$$MA = enol \qquad (9')$$

$$I_2 + enol = IMA + I^- + H^+ \qquad (9'')$$

where MA ≡ $CH_2(COOH)_2$, enol ≡ $(OH)_2C=CHCOOH$, and IMA = $CHI(COOH)_2$. By making a steady-state approximation on the enol,[27] one obtains a rate law of the form

$$v_9 = -\frac{d[I_2]}{dt} = \frac{k_9' k_9''[MA][I_2]}{k_9' + k_9''[I_2]} \equiv \frac{k_9[MA][I_2]}{1 + C_9[I_2]} \qquad (V9)$$

Leopold and Haim[28] have studied reaction 9 and have obtained a somewhat more complex rate law. Furrow[11] has investigated this reaction under conditions closer to those of the BR system. Using his data, we obtain $k_9 = (5/2)16\ M^{-1}\ s^{-1} = 40\ M^{-1}\ s^{-1}$, where the 5/2 is a stoichiometric factor resulting from the presence of iodate and $C_9 = 10^4\ M^{-1}$. If malonic acid is replaced by methylmalonic acid, the experiments of Furrow[11] yield $k_9^{MMA} = (5/2)6.4\ M^{-1}\ s^{-1} = 16\ M^{-1}\ s^{-1}$ and $C_9^{MMA} = 10^5\ M^{-1}$.

Reaction 10. The importance of this essentially irreversible step in the hydrogen peroxide–iodine reaction has been shown by Liebhafsky,[29] who gives rate law V10 at 25 °C with $k_{10} = 37\ M^{-1}\ s^{-1}$.

$$v_{10} = -d[HOI]/dt = k_{10}[H_2O_2][HOI] \qquad (V10)$$

Calculations

Method. The rate equations derived from eq V1–V10 were augmented by flow terms $k_0[X]_0 - k_0[X]$ for each species X, where k_0 is the flow rate (reciprocal of the residence time) and the input concentration $[X]_0$ is the concentration that species X would have if all the chemicals were combined in a single input flow without reaction. For each experimental simulation a set of initial concentrations in the reactor $[X]_i$, a flow rate k_0 and input concentrations $[X]_0$ had to be supplied. For tests of hysteresis behavior, a series of calculations was done in which a parameter (k_0 or an $[X]_0$) was varied and the $[X]_i$ values for each calculation were taken as the steady-state concentrations from the previous one.

The equations were integrated numerically by using Hindmarsh's version[30] of the Gear method[31] for stiff differential equations. The equations are apparently quite stiff and, especially for high $[MA]_0$, the computing time required to attain a steady state was sometimes as long as 20–30 min for a single simulation on the Brandeis University PDP-10 computer.

Since no pH changes greater than 0.01 were observed experimentally, in the simulations $[H^+]$ was held fixed. The total manganese $[Mn^{2+}] + [MnOH^{2+}]$ and the total organic species [MA] + [IMA] are also constants. We thus had nine variable concentrations in the model: $[IO_3^-]$, $[I^-]$, $[I_2]$, $[HIO_2]$, [HOI], $[IO_2]$, $[MnOH^{2+}]$, [HOO], and [MA]. Oxygen was treated as an inert product, though its concentration could be obtained if desired from the results of the simulations.

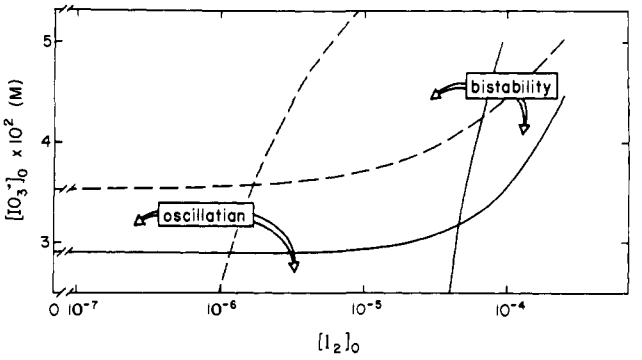

Figure 1. Experimental (—) and calculated (---) "cross-shaped phase diagram" in the $[IO_3^-]_0$–$[I_2]_0$ constraint space. Other constraints held constant at $[H_2O_2]_0 = 0.33$ M, $[CH_2(COOH)_2]_0 = 0.0015$ M, $[H^+]_0 = 0.056$ M, $[Mn^{2+}]_0 = 0.004$ M, residence time = 156 s, and $T = 25$ °C.

Results of Calculations. In Figure 1 we present the experimentally determined[12,15] and calculated phase diagrams of the system in the $[I_2]_0$–$[IO_3^-]_0$ constraint plane. Qualitatively, the calculation predicts the cross-shaped topology of the diagram. The position of the computed cross point, where the monostable, bistable, and oscillatory regions join, is in nearly quantitative agreement with the experimentally observed value for $[IO_3^-]_0$. However this point is shifted to an iodine flow nearly 30 times too small.

Another computed section of the phase diagram, this time in the $[IO_3^-]_0$–$[MA]_0$ plane (Figure 2a), is compared with the corresponding experimental phase diagram[12,15] (Figure 2b). The shape of the calculated and experimental plots differ significantly, though certain key features such as the dependence of the period on the malonic acid flow, are in good agreement. The model predicts that at certain $[IO_3^-]_0$ values, oscillations persist even as $[MA]_0$ is decreased to zero. This behavior has not been observed experimentally.

One remarkable feature of the BR reaction in a flow reactor is the inverse regulation of $[I_2]$. For a given set of values of the other constraints, at low iodine flows ($[I_2]_0$) the system attains a steady state (denoted SSII) in which the iodine concentration ($[I_2]_{SSII}$) considerably exceeds $[I_2]_0$, while at high values of $[I_2]_0$, the system reaches a steady state (SSI) in which $[I_2]_{SSI} < [I_2]_0$. This behavior is shown in Figure 3. Above a critical value of $[I_2]_0$ a transition occurs from SSII to SSI, directly or through an oscillatory region, so that an increase in the iodine input flow results in a net *drop* in the iodine concentration in the reactor!

As Figure 3 shows, the calculation gives semiquantitative agreement with the observed inverse regulation of iodine for both the steady state I_2 concentrations and locations of the SSII → SSI transitions. However, at the other end of the hysteresis loop, where the system jumps from SSI to SSII as $[I_2]_0$ is decreased, the calculated transition points occur at values of $[I_2]_0$ much lower than observed, i.e., the model makes SSI much too stable.

We note that the slight overestimate of the calculated $[I_2]_{SSII}$ values could probably be corrected by including in the model the experimentally observed evaporation of iodine from the reactor. However, in view of the more serious discrepancies between theory and experiment, such "fine tuning" was not deemed justified.

The two steady states differ not only in the concentrations of I_2, but in all other species concentrations as well. In Table I we list the concentrations of major species in the two steady states for a set of constraints in the bistable region near the cross point. SSI is characterized by lower concentrations of $MnOH^{2+}$ and of all iodine containing species except I^-. This state, a true steady state in the flow system, corresponds to the nonradical pseudo

(27) Strictly speaking, under flow conditions the steady-state calculation must also take into account the rate of flow of the enol out of the reactor. However, the effect of this additional term is negligible so long as $k_0 << k_{-9}'$. For the experiments under discussion in this work, k_0/k_{-9}' is typically about 3×10^{-4}.

(28) Leopold, K.; Haim, A. *Int. J. Chem. Kinet.* **1977**, *9*, 83–95.
(29) Liebhafsky, H. A. *J. Am. Chem. Soc.* **1932**, *54*, 3504–3508.
(30) Hindmarsh, A. G. "Gear: Ordinary Differential Equation Solver", Tech. Rept. No. UCM-30001, Rev. 2, Lawrence Livermore Laboratory, 1972.
(31) Gear, C. W. "Numerical Initial Value Problems in Ordinary Differential Equations"; Prentice-Hall: Englewood Cliffs, N.J., 1971; Chapter 11.

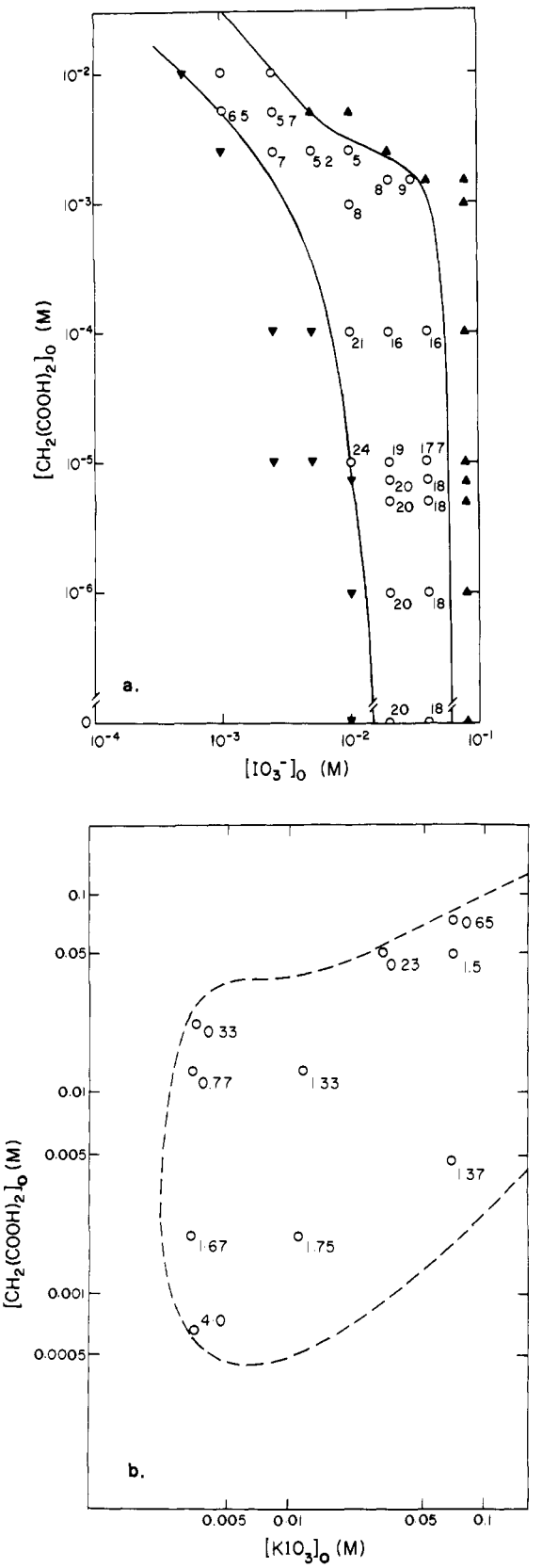

Figure 2. Computed (a) and experimental (b) phase diagram in the $[CH_2(COOH)_2]_0$–$[IO_3^-]_0$ constraint space with $[I_2]_0 \equiv 0$, all other constraints as in Figure 1: ▼, SSI; ▲, SSII; O, oscillations with period in minutes.

steady state referred to by Noyes and Furrow.[10c] The radical steady state SSII shows concentrations of the radical species IO_2 and $MnOH^{2+}$ roughly 4 orders of magnitude higher than in SSI. Figure 4 allows comparison between the concentration jump in the oscillatory state and the neighboring steady-state concentrations in the bistable region. It clearly shows that during oscillations the system essentially jumps periodically between these steady-state critical values.

In Figure 5a we show a projection in the iodide sensitive electrode potential–$[I_2]$ response plane of the experimental limit cycle.[12] The corresponding calculated projection in the $[I^-]$–$[I_2]$

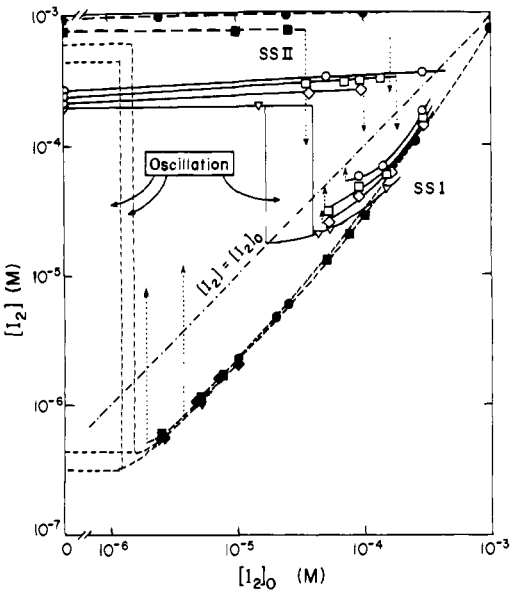

Figure 3. Calculated and experimental "inverse regulation" of iodine. Steady state iodine concentration $[I_2]$ vs. input-flow concentration $[I_2]_0$. Arrows indicate spontaneous transitions between states for different $[IO_3^-]_0$: 0.047 M, ● (calcd), O (exptl); 0.040 M, ■ (calcd), □, (exptl); 0.035 M, ♦, (calcd), ◇ (exptl); 0.030 M, ▼, (calcd), △, (exptl). All other constraints are as in Figure 1.

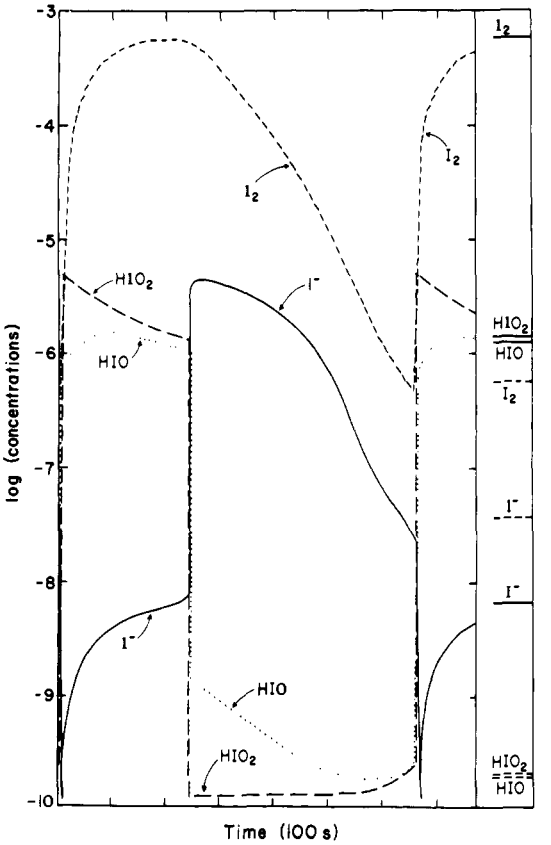

Figure 4. Computed oscillations of $[I^-]$, $[I_2]$, [HIO], and $[HIO_2]$ for $[IO_3^-]_0 = 0.035$ M and $[I_2]_0 = 10^{-6}$ M and in the right-hand column SSI (---) and SSII (—) concentrations of the same species for $[IO_3^-]_0 = 0.038$ M and $[I_2]_0 = 2.8 \times 10^{-6}$ M, a neighboring bistable composition. All other constraints are as in Figure 1.

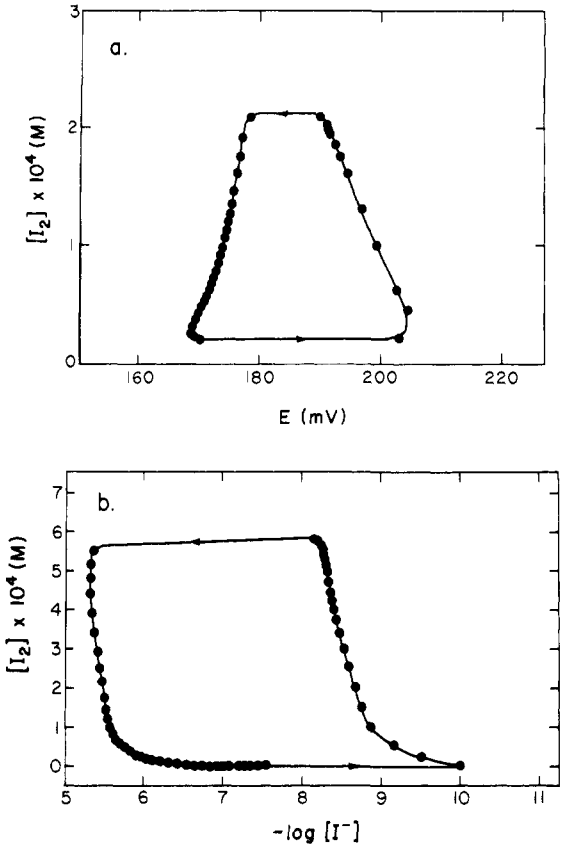

Figure 5. Projection of the limit cycle (a) in the $[I_2]$–Pt electrode potential plane for the experimentally observed oscillating composition on Figure 1 and (b) in the $[I_2]$–$[I^-]$ plane for a calculated oscillatory state on Figure 1. The time interval between points is 12 s.

plane is shown for comparison in Figure 5b. The points are equidistant in time to afford an idea of the relative rates of change at different points on the cycle, which further emphasizes the similarities between the computed and experimental projections of the limit cycle. Finally, if we compare our computed oscillograms of I^- and I_2 (Figure 4) with those derived by Roux and Vidal[13] from their experimental data (although the conditions are not identical), we observe qualitative agreement between the experimental and calculated phases of these species. During a single period of oscillation, the iodine concentration reaches a maximum as iodide increases by several orders of magnitude. Then iodine decreases slowly with iodide, followed by a rapid increase in iodine as the iodide concentration suddenly drops by several orders of magnitude to a minimum. The iodide then increases slightly before undergoing a sharp increase as iodine again reaches its maximum concentration.

Variation of Rate Constants. A number of tests were made of the sensitivity of the model to changes in the expendable parameters. These variations in the k's were carried out primarily for the conditions shown in the cross-shaped $[IO_3^-]_0$–$[I_2]_0$ phase diagram section of Figure 1. Each rate constant was varied by a factor of at least 10.

Decreasing k_2 shifts the point of transition from the oscillatory state to SSII toward lower values of $[IO_3^-]$. Malonic acid and iodate consumption are increased and $[I_2]_{SSII}$ also increases significantly.

An increase in k_{-4}, the rate of disproportionation of the IO_2 radicals, somewhat surprisingly has little effect on the stability of SSII, though it does cause a decrease in $[I_2]_{SSII}$.

The model appears most sensitive to changes in k_5 and k_6. As k_5 is increased, the transition from oscillations to SSII shifts to lower $[IO_3^-]_0$ and $[I_2]_{SSII}$ increases nearly proportionally to k_5. Increasing k_6 also decreases the stability of the oscillatory state relative to SSII, thereby lowering the critical $[IO_3^-]_0$ for the transition. Higher k_6 values, however, tend to lower $[I_2]_{SSII}$ slightly.

Methylmalonic Acid. As noted above, the BR reaction with methylmalonic acid may be simulated by replacing the values of k_9 and C_9 for MA by Furrow's[11] corresponding values for MMA. Using the same conditions reported by Briggs and Rauscher[2] (no flow, $[IO_3^-]_i = 0.067$ M, $[MA]_i = 0.050$ M, $[Mn^{2+}]_i = 0.0067$ M, $[H_2O_2]_i = 1.20$ M, $[H^+]_i = 0.035$ M), we obtained oscillations with both the MA and MMA parameters. The periods of oscillation were $I_{MA} = 140$ s and $I_{MMA} = 400$ s. Experimentally, we observe an increase of a factor of about 6 on replacing malonic by methylmalonic acid.

Discussion

The mechanism presented here bears strong resemblances to the models of the BR system developed independently by Cooke[9] and by Noyes and Furrow.[10] Cooke's mechanistic discussion includes all of the steps in our model as well as a large number of additional reactions involving such radical species as I, IO, and OH. No rate constants are given, and no attempt is made at calculating any kinetic behavior. The steps of Noyes and Furrow's scheme are identical with ours, except that they treat reactions 9′ and 9″ separately, so that the enol becomes an additional independent species.

While many of our rate constants, being experimentally determined, are the same as those used by Noyes and Furrow, we differ in the values chosen for several of the expendable parameters, most notably k_4, k_{-4}, and k_5. In spite of a difference of more than 4 orders of magnitude in k_5, we have verified that our model does give oscillations under the conditions of Noyes and Furrow's calculation. We believe that the much lower concentrations of HIO_2 and IO_2 found in our simulations lie closer to the actual values.

Some insight into the behavior of the system may be gleaned by examining the velocities of the individual steps in the mechanism. We find, for example, that in all cases $v_2 < v_4$ when the system is in the nonradical steady state SSI, with the inequality reversed in SSII. Furthermore, the shift from high $[I^-]$, low $[I_2]$, and low radical concentrations to low $[I^-]$ and high concentrations of the other species occurs just as v_4 begins to exceed v_2. Thus, the switching between the nonradical and radical regimes depends upon whether or not $[I^-]$ is high enough so that HIO_2 reacts preferentially in the nonradical step (2) rather than in the radical autocatalytic step (4). This switching takes place at a critical iodide value given by $[I^-]_c = (k_4/k_2)[IO_3^-] = (3.7 \times 10^7)[IO_3^-]$, which is consistent with the transition shown in Figure 4.

All the component reactions with the exception of (1) proceed more rapidly in the radical state (or the radical portion of the oscillation period) than in the nonradical state. Interestingly, in the radical regime, the order of some of the principal reaction velocities is $v_{10} > v_4 > v_2 > v_3 > v_9$, while in the nonradical state these velocities fall in exactly the opposite order, though they all drop by several orders of magnitude.

The rates of eq 4, 6, and 7 are very strongly coupled, with $v_6 = v_7 = {}^1/_2 v_4$ at all times to an accuracy of better than 1%. This observation first suggested to us that either step 4 or step 6 was rate determining for the overall sequence (4) + 2((6) + (7)) or

$$IO_3^- + 2H_2O_2 + H^+ = HIO_2 + 2HOO + H_2O \quad (14)$$

However, testing this hypothesis showed that the reaction profile was sensitive to all three rate parameters k_4, k_{-4}, and k_6.

On further consideration, we recognized that the coupling of v_4, v_6, and v_7 implies only that $[MnOH^{2+}]$ and $[IO_2]$ maintain pseudo-steady-state values throughout the course of the reaction. Setting

$$d[IO_2]/dt = 0$$

we obtain

$$[IO_2]_{pss} = \frac{k_6[Mn^{2+}]}{4k_{-4}}\left[\left(\frac{1 + 16k_4k_{-4}[H^+][HIO_2][IO_3^-]}{k_6^2[Mn^{2+}]^2}\right)^{1/2} - 1\right] \quad (15)$$

The rate of production of HIO_2 via process 14 may be written as

$$\frac{d[HIO_2]}{dt} = \frac{1}{2}\frac{d[HOO]}{dt} = \frac{1}{2}k_7[H_2O_2][MnOH^{2+}] = \frac{1}{2}k_6[Mn^{2+}][IO_2] \quad (16)$$

where the last equality results from setting $d[MnOH^{2+}]/dt = 0$. Two limiting cases arise, depending upon the relative sizes of the terms $16k_4k_{-4}[H^+][HIO_2][IO_3^-]$ and $k_6^2[Mn^{2+}]^2$ in eq 15. If step 4 is rate determining so that the latter term is much larger, then we find

$$[IO_2]_{pSS} \approx (2k_4/k_6)[H^+][HIO_2][IO_3^-]/[Mn^{2+}] \quad (17)$$

and, substituting in (16)

$$d[HIO_2]/dt = k_4[H^+][HIO_2][IO_3^-] \quad (18)$$

The sequence then produces HIO_2 autocatalytically in a process also catalyzed by manganous ion. On the other hand if step 6 is ratedetermining, then the pseudo-steady-state value of iodine dioxide is given by eq 19 and 20, where $K_4 = k_4/k_{-4}$. We still

$$[IO_2]_{pSS} \approx (K_4[H^+][HIO_2][IO_3^-])^{1/2} \quad (19)$$

$$d[HIO_2]/dt = \frac{1}{2}k_6K_4^{1/2}[Mn^{2+}]([H^+][HIO_2][IO_3^-])^{1/2} \quad (20)$$

have autocatalysis in HIO_2 but now of a lower order and catalyzed by manganous ion. On examining the values of the rate constants and species concentrations during the course of an oscillation or in the two steady states (see Table I), we observe that the relative magnitudes of the two terms in eq 15 are interchanged as the system switches from the radical to the nonradical regime. Thus neither approximation holds over the entire course of the reaction, and the only permissible "simplification" would be to combine eq 4, 6, and 7 into the single autocatalytic process (14) with a rate law derived from eq 15 and 16.

While the mechanism presented here succeeds in predicting many of the dynamic features of the system over a wide range of constraint values, several major discrepancies remain between theory and experiment in the BR system. Minor quantitative differences could probably be improved by further manipulation of the rate constants, but all the major qualitative disagreements appear to be attributable to a common problem which is unlikely to be resolved by additional refinement of the expendable parameters. A more drastic solution is required.

As we see in Figures 1 and 3, wherever there are large differences between the simulated and experimental dynamics of the system, these discrepancies are associated with an overestimate of the region of stability of SSI; the model makes the nonradical state too stable. This is especially clear in the lower left part of Figure 3.

One way to destablize the nonradical SSI in the calculation is to "push" the system toward the radical state by producing an appropriate chemical species. Although varying certain rate constants (e.g., increasing k_4, decreasing k_5) will serve this purpose, this procedure also changes the system in other ways, destroying the agreement between simulation and experiment at other points. One highly suggestive result is that introducing an input flow of iodous acid ($[HIO_2]_0 = 10^{-6}$ M) into the simulation decreases the range of stability of SSI and increases the iodine minimum in the oscillatory state without noticeably affecting the other calculated results. This observation suggests that augmentation of the mechanism by steps which produce HIO_2 at a sufficient rate without perturbing the rest of the model too greatly might resolve most if not all of the remaining discrepancies between theory and experiment. A possible candidate is

$$H_2O_2 + IO_3^- + H^+ = HIO_2 + H_2O + O_2 \quad (21)$$

though the rate given by Liebhafsky in 1931[32] for this reaction would make it much too slow to produce iodous acid at the appropriate rate. Further experimental investigation of this reaction may be in order.

The validity of a model of such complexity is credible only if *several* major experimental features are reproduced. The fact that the mechanism presented here predicts not only oscillations but also bistability with the observed inverse regulation of iodine and the dependence of the period on malonic acid all suggest that this scheme does indeed account for the kinetic skeleton of the Briggs–Rauscher system. The computational effort involved has been considerable and important gaps remain, but in view of the agreement achieved both with experiment and with other models independently arrived at, it appears that mechanistic understanding of the Briggs–Rauscher reaction has taken a large step forward.

Acknowledgment. This work was supported by National Science Foundation Grant CHE7905911. We are extremely grateful to Professors R. M. Noyes and S. D. Furrow for communicating their results to us prior to publication. We thank Professor Kenneth Kustin for a critical reading of the manuscript.

(32) Liebhafsky, H. A. *J. Am. Chem. Soc.* **1931**, *53*, 896–911.

Olefin Rearrangement Resulting from the Gas-Phase KrF Laser Photolysis of $Cr(CO)_6$

William Tumas, Barbara Gitlin, Alan M. Rosan, and James T. Yardley*

Contribution from Corporate Research and Development, Allied Corporation, Morristown, New Jersey 07960. *Received January 16, 1981*

Abstract: We have found that irradiation of $Cr(CO)_6$–1-butene mixtures in the gas phase with a KrF laser (248 nm) results in the efficient (yield ~0.2) isomerization of 1-butene to 2-butene, in marked contrast to results in solution. The primary photochemical yield is independent of 1-butene pressure and of $Cr(CO)_6$ pressure over wide pressure ranges. Secondary photochemical processes are also found, the importance of which depends upon 1-butene pressure. We also report yields of species $Cr(CO)_m(PF_3)_{6-m}$ resulting from irradiation of $Cr(CO)_6$–PF_3 mixtures at 248 nm. At high dilution [$Cr(CO)_6$:PF_3 = 2×10^{-3}], we find relative yields of 0.10, 0.14, 0.73, and 0.03 for $Cr(CO)_2(PF_3)_4$, $Cr(CO)_3(PF_3)_3$, $Cr(CO)_4(PF_3)_2$, and $Cr(CO)_5PF_3$, respectively. These results suggest a high degree of fragmentation following optical excitation at 248 nm. We present a reasonable kinetic model to explain the observed isomerization of butene in which a primary photofragment, probably $Cr(CO)_3$ or $Cr(CO)_2$, is the active species.

I. Introduction

It has long been recognized that the photoexcitation of metal carbonyl compounds may result in species which are active for photocatalytic or photoassisted processes.[1-3] For species of the form $M(CO)_n$, where M is a transition metal, it has generally been accepted that the primary photochemical process involves the

(1) M. S. Wrighton, *Chem. Rev.*, **74**, 401 (1974).

0002-7863/82/1504-0055$01.25/0